

Few-photon-level two-dimensional infrared imaging by coincidence frequency upconversion

Kun Huang, Xiaorong Gu, Haifeng Pan, E Wu, and Heping Zeng

Citation: *Appl. Phys. Lett.* **100**, 151102 (2012); doi: 10.1063/1.3703610

View online: <http://dx.doi.org/10.1063/1.3703610>

View Table of Contents: <http://apl.aip.org/resource/1/APPLAB/v100/i15>

Published by the [American Institute of Physics](#).

Related Articles

A readout for large arrays of microwave kinetic inductance detectors
Rev. Sci. Instrum. **83**, 044702 (2012)

Channelling optics for high quality imaging of sensory hair
Rev. Sci. Instrum. **83**, 045001 (2012)

A spherical crystal imager for OMEGA EP
Rev. Sci. Instrum. **83**, 033107 (2012)

New Products
Rev. Sci. Instrum. **83**, 039501 (2012)

Subwavelength optical absorber with an integrated photon sorter
APL: Org. Electron. Photonics **5**, 73 (2012)

Additional information on *Appl. Phys. Lett.*

Journal Homepage: <http://apl.aip.org/>

Journal Information: http://apl.aip.org/about/about_the_journal

Top downloads: http://apl.aip.org/features/most_downloaded

Information for Authors: <http://apl.aip.org/authors>

ADVERTISEMENT



PFEIFFER  **VACUUM**

Complete Dry Vacuum Pump Station
for only **\$4995** — HiCube™ Eco

800-248-8254 | www.pfeiffer-vacuum.com

Few-photon-level two-dimensional infrared imaging by coincidence frequency upconversion

Kun Huang, Xiaorong Gu, Haifeng Pan, E Wu,^{a)} and Heping Zeng

State Key Laboratory of Precision Spectroscopy, East China Normal University, Shanghai 200062, China

(Received 20 December 2011; accepted 29 March 2012; published online 12 April 2012)

We demonstrate few-photon-level infrared imaging at 1040 nm by coincidence frequency upconversion with a high conversion efficiency of 33.5%. By synchronous pulse pumping at 1549 nm, the infrared object image was spectrally upconverted into the visible regime. The upconverted image was captured by a silicon electron multiplying charged coupled device without any scanning devices, thus gaining in simplicity and speed. The imaging sensitivity was improved by reducing the background noise with coincidence pulsed pumping at long wavelength. © 2012 American Institute of Physics. [<http://dx.doi.org/10.1063/1.3703610>]

Ultra-sensitive infrared imaging has numerous applications in biology, astronomy, medical diagnosis, and two-dimensional (2D) infrared spectroscopy.^{1,2} Typically, the infrared imaging can be achieved by a linear InGaAs photodiode array. However, suffering from the severe dark current, the sensitivity of such detectors is largely limited.³ Even though liquid-nitrogen-cooling can provide a solution for a smaller dark current, the additional cryogenic cooling device reduces the feasibility for wide applications. Unlike in the infrared regime, imaging in the visible regime can be readily implemented by silicon charged coupled devices (CCDs) with high resolution and high efficiency. Moreover, recent progresses in sensor technology have led to the development of electron multiplying CCDs (EMCCDs) capable of single-photon detection. By leveraging the high sensitivity of EMCCDs, ultra-sensitive infrared imaging can be expected with nonlinear frequency conversion of the infrared electric field to the visible spectral region.⁴⁻⁶ This technique typically requires a strong pump field to obtain unitary frequency upconversion in a transparent crystal with large nonlinearity. Recently, frequency upconversion of infrared images at 765 nm was demonstrated by intra-cavity enhanced frequency upconversion.⁷ However, the strong continuous-wave pump field would inevitably bring about severe background noise due to parasitic nonlinear interactions, thus largely lowering the sensitivity of low-level-light infrared imaging.^{8,9} Pulsed pump field could be employed as a coincident gate for upconverting the infrared signal with high efficiency and low noise.^{10,11} Benefited from the intense peak power of the pulsed field, high conversion efficiency could be achieved with a modest average pump power, thus loosening the restriction for the available pump power.^{4,10} Additionally, the background noise induced by the strong pump can be effectively reduced due to the pulsed excitation.

In this Letter, we demonstrated few-photon-level infrared imaging at 1040 nm based on frequency upconversion pumped by synchronized pulses at 1549 nm. The imaging photons were from the sum frequency generation (SFG) of

the signal photons with the pumping pulse in a periodically poled lithium niobate (PPLN) crystal with a conversion efficiency of about 33.5% and then detected by a high performance EMCCD. Thanks to the short time window of the synchronized pump pulse together with long-wavelength pumping scheme, the imaging sensitivity was improved effectively by reducing the background noise. Moreover, in contrast to the imaging method with time-consuming x,y-scanning,¹² such upconversion imaging system produced a full 2D image, thus gaining in simplicity and speed.

As shown in Fig. 1, the experimental setup consisted of two parts: synchronization laser system and upconversion imaging system. The synchronization laser system was composed of two fiber lasers arranged in master-slave cavity configuration. The master was a mode-locked ytterbium-doped fiber laser (YDFL) operating at 19.1 MHz. To satisfy the quasi-phase-matching bandwidth of the PPLN crystal (0.3 nm),¹³ a narrow spectrum signal source at 1040 nm was obtained by filtering the output of YDFL with a 0.3-nm bandwidth fiber Bragg grating (FBG). The corresponding pulse duration was measured to be 6 ps from the autocorrelation trace. The FBG transmission was then amplified by an ytterbium-doped fiber amplifier before being injected into an erbium-doped fiber laser (EDFL) for achieving synchronous mode-locking by means of cross-phase modulation effect. In order to obtain an appropriate narrow spectrum of EDFL, a

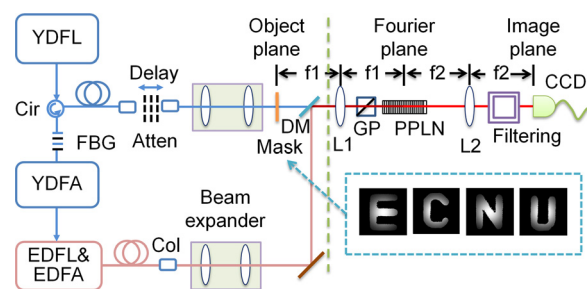


FIG. 1. Experimental setup for infrared imaging by coincidence frequency upconversion. YDFL, ytterbium-doped fiber laser; YDFA, ytterbium-doped fiber amplifier; EDFL, erbium-doped fiber laser; EDFA, erbium-doped fiber amplifier; Cir, circulator; Col, collimator; Atten, attenuator; DM, dichroic mirror; GP, Glan prism; PPLN, periodically poled lithium niobate crystal; CCD, charged coupled device. Transmission masks were shown in the bottom-right corner.

^{a)}Authors to whom correspondence should be addressed. Electronic addresses: ewu@phy.ecnu.edu.cn and hpzeng@phy.ecnu.edu.cn.

fiber band-pass filter with a 3-nm bandwidth was placed in the laser cavity. The output of the EDFL was then amplified by an erbium-doped fiber amplifier to 40.0 mW as the pump source. The corresponding spectrum centered at 1549 nm with a bandwidth of 0.7 nm. For improving the conversion efficiency, the pulse duration of the pump was engineered to be about 16 ps, which was longer than that of the signal, so that the pump pulse could be synchronously adjusted to tightly enwrap the signal pulse.^{10,11} Then, the synchronized beams of signal and pump were expanded into space after fiber collimators. The (e^{-2} intensity) beam radii of signal and pump were measured to be about 1.7 and 1.0 mm, respectively. The signal beam then coherently illuminated onto a transmission mask with characters “E,” “C,” “N,” and “U” to form the object beams. The corresponding object beams were shown in the bottom-right corner of Fig. 1, and the size of each squared image was 4 mm. The object beam was in combination with the synchronized pump beam by a dichroic mirror and sent into the upconversion imaging system. Lens L1 ($f_1 = 250$ mm) and L2 ($f_2 = 300$ mm) were arranged in 4-f imaging configuration as shown in Fig. 1, where the mask was located at the object plane and the CCD detector was located at the image plane. For facilitating the type I quasi-phase matching of the PPLN crystal, a Glan prism was fixed in front of the crystal to enforce the right polarization of the two beams. Lens L1 was an achromatic doublet lens for minimizing the chromatic aberration to focus the pump and object beams with optimized spatial mode matching. The Fourier plane of the 4-f imaging system was located at the center of the 50-mm-long PPLN crystal. The temperature of the crystal was optimized at 104.3 °C for the grating period of 11.0 μm . The temperature was high enough to avoid photorefractive effects.¹⁴ The infrared object beam interacted with the pump beam, and was upconverted through SFG to generate the visible image at 622 nm.

Before injecting on the detector, the collimated upconverted light was steered in sequence through a prism for chromatic dispersion, and a band-pass interference filter for suppressing the background noise. The transmittance of the whole filtering was estimated to be 80%. With strong signal light illuminating the mask, the power detection efficiency was measured to be 41.2%, 35.7%, 44.8%, and 41.3% for the character “E,” “C,” “N,” and “U,” respectively. By correcting the power detection efficiency for the measured optical loss, the conversion efficiency for each character could be inferred respectively to 30.8%, 26.7%, 33.5%, and 30.9% in the image upconversion process. The slight variation of the conversion efficiency was due to the different Fraunhofer diffraction patterns of characters at the Fourier plane. Figures 2(a)–2(d) displayed the distribution of the electric field at the Fourier plane. Since only the low spatial frequency components located at the center of the focused pump beam could be efficiently upconverted with sufficient pump intensity, the pump beam worked as a Gaussian spatial filter. Figures 2(e)–2(h) showed the filtered Fourier transformation patterns by the pump beam. Without the mask, the conversion efficiency could reach 56.6% because the signal beam in Gaussian shape was more concentrated at the Fourier plane. The upconverted images were shown in Figs. 2(m)–2(p), from which the characters could be seen clearly but with blurred

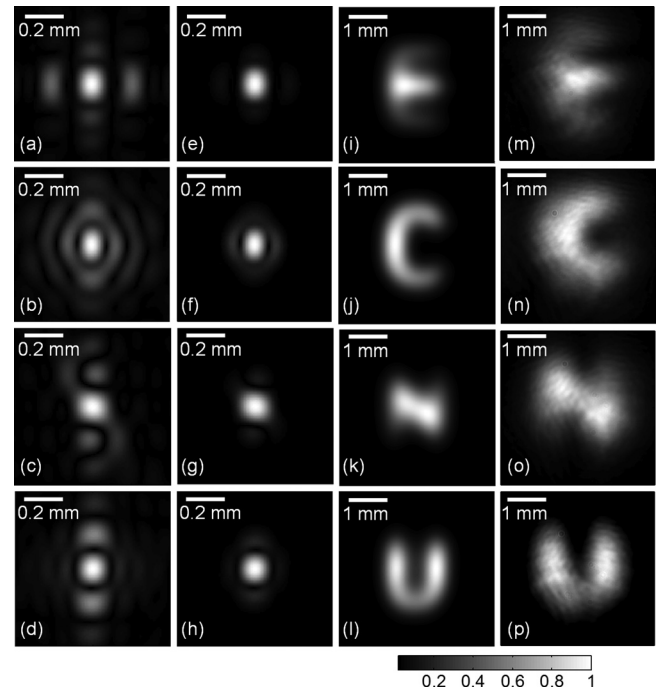


FIG. 2. Distribution of electric field of the signal beams at the Fourier plane without [(a)–(d)] and with [(e)–(h)] the Gaussian pump beam. Theoretical simulation of upconverted images with strong object beam light [(i)–(l)] and experimental results [(m)–(p)].

edges. The image distortion was ascribed to the intrinsic point spread function (PSF) effect in the upconversion imaging system. For the coherent imaging in our experiment, the upconverted field at the image plane can be described as a convolution between the ideal geometrical-optics predicted image field, which is a scaled copy of the object field, and the PSF of the imaging system.⁷ The main part of PSF could be expressed by

$$PSF \propto e^{-\frac{x^2+y^2}{\left(\frac{\lambda_{up}/2}{\pi\omega_0}\right)^2}}, \quad (1)$$

where the λ_{up} is the wavelength of the upconverted field, ω_0 is the radius of the pump beam at the Fourier plane. Note that the size of the Gaussian beam defines the shape of the PSF and thus the imaging resolution. With the parameters in our experimental conditions, the theoretical upconverted images were shown in Figs. 2(i)–2(l). The effect of PSF smearing out the edges of the images could be observed clearly, consisting with the experimental results.

In order to demonstrate the competence of ultra-sensitive low-light-level infrared imaging by the frequency upconversion system, the object beam was attenuated to the few-photon level. The average photon numbers per pulse for the object beam “E,” “C,” “N,” and “U” were estimated to be 1.9, 2.0, 2.4, and 2.6, respectively. Then, the visible photons of the frequency upconverted images were registered by an EMCCD (Andor iXon3 897), which was thermoelectrically cooled to -85 °C to lower the dark noise. The EMCCD was a silicon-based semiconductor chip bearing 512×512 pixels, and the pixel size of $16 \times 16 \mu\text{m}$ was suitable for high spatial resolution imaging. For the object beam “E,” “C,” “N,” “U,” we set the integration time of 30, 30, 35, and 30 s,

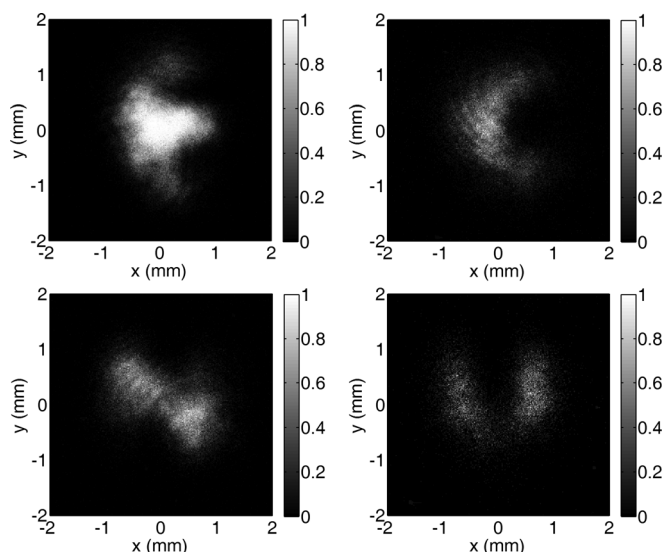


FIG. 3. Measured upconverted images with few-photon-level object beam light.

and the accumulation number of 50, 50, 50, and 30, respectively. Thanks to the pulsed pump field, the background noise induced by the parametric fluorescence was effectively reduced.^{4,11} Combined with the long-wavelength pumping, the background noise was normally 1.5×10^3 cps (counts per second),¹⁰ meaning that the noise probability per pulse was about 8×10^{-5} . Such a low noise probability guaranteed that the few-photon-level infrared imaging could be achieved by eliminating the smearing effect of the background counts. As shown in Fig. 3, the obtained images were similar to those with strong signal light shown in Figs. 2(m)–2(p). In order to improve the resolution, it would be better to have a larger pump beam profile or stronger focusing of the infrared image. According to Eq. (1), for improving the resolution of the imaging process, it is necessary to have a larger pump beam to wrap spatial components of the object image at the Fourier plane as much as possible. However, increase of the pump beam spot diameter would lead to the decrease of the pump intensity (assuming constant power), therefore reduce the conversion efficiency. On the other hand, stronger focusing of the object image is limited by the angular acceptance parameter of the long nonlinear crystal. Thus, a trade-off optimization of the two parameters should be concerned. The problem can be solved by a higher pump power with an enlarged beam size and by employing a short nonlinear crystal with a larger accepted angle. Normally, for a specific upconversion system with particular pump and phase match condition, the PSF should be well defined. Therefore, it may be possible with a suitable choice of PSF to deconvolve the upconverted image and obtain a sharper image.⁷ Recent

research showed that it is also possible to achieve better resolution by the image upconversion of incoherent light.¹⁵

In summary, we demonstrated few-photon-level full 2D infrared imaging at 1040 nm by means of efficient and low-noise frequency upconversion. The background noise induced by the strong pump was effectively reduced by the synchronized pulsed excitation of the 1549 nm pump source, as well as the long-wavelength pumping. The visible photons of upconverted images were captured by the silicon EMCCD with high sensitivity and resolution. Optimization of the beam sizes of the pump and signal, a choice of short crystal but with high nonlinear coefficient and amplification of the pump power, are expected to further increase the conversion efficiency and improve the resolution. Such all-optical upconversion imaging system may find promising applications that require ultra-sensitive infrared imaging such as 2D infrared spectroscopy for characterizing molecular systems. Moreover, the presented technique can be extended to mid-infrared regime where the simple and efficient image detection is difficult to perform with existing detector technologies.¹⁶

This work was funded in part by National Natural Science Fund of China (10990101, 60807027, 60907043, and 91021014), Key project sponsored by the National Education Ministry of China (109069), Research Fund for the Doctoral Program of Higher Education of China (200802691032, 20090076120024), Innovation Program of Shanghai Municipal Education Commission (09ZZ47), and ECNU Reward for Excellent Doctors in Academics.

¹M. J. Nee, R. McCanne, K. J. Kubarych, and M. Joffre, *Opt. Lett.* **32**, 713 (2007).

²L. Ma, O. Slattery, and X. Tang, *Opt. Express* **17**, 14395 (2009).

³A. P. Vandevender, and P. G. Kwiat, *J. Mod. Opt.* **51**, 1433 (2004).

⁴H. Dong, H. Pan, Y. Li, E Wu, and H. Zeng, *Appl. Phys. Lett.* **93**, 071101 (2008).

⁵R. T. Thew, H. Zbinden, and N. Gisin, *Appl. Phys. Lett.* **93**, 071104 (2008).

⁶S. Tanzilli, W. Tittel, M. Halder, O. Alibart, P. Baldi, N. Gisin, and H. Zbinden, *Nature* **437**, 116 (2005).

⁷C. Pedersen, E. Karamehmedović, J. S. Dam, and P. T. Lichtenberg, *Opt. Express* **17**, 20885 (2009).

⁸M. A. Albota and F. N. C. Wong, *Opt. Lett.* **29**, 1449 (2004).

⁹H. Pan, H. Dong, H. Zeng, and W. Lu, *Appl. Phys. Lett.* **89**, 191108 (2006).

¹⁰X. Gu, K. Huang, Y. Li, H. Pan, E Wu, and H. Zeng, *Appl. Phys. Lett.* **96**, 131111 (2010).

¹¹K. Huang, X. Gu, M. Ren, Y. Jian, H. Pan, G. Wu, E Wu, and H. Zeng, *Opt. Lett.* **36**, 1722 (2011).

¹²D. Stothard, M. Dunn, and C. Rae, *Opt. Express* **12**, 947–955 (2004).

¹³H. Takesue, E. Diamanti, C. Langrock, M. M. Fejer, and Y. Yamamoto, *Opt. Express* **14**, 13067 (2006).

¹⁴P. Xu, S. H. Ji, S. N. Zhu, X. Q. Yu, J. Sun, H. T. Wang, J. L. He, Y. Y. Zhu, and N. B. Ming, *Phys. Rev. Lett.* **93**, 133904 (2004).

¹⁵J. S. Dam, C. Pedersen, and P. T. Lichtenberg, *Opt. Lett.* **35**, 3796 (2010).

¹⁶K. J. Kubarych, M. Joffre, A. Moore, N. Belabas, and D. M. Jonas, *Opt. Lett.* **30**, 1228 (2005).